IOP Publishing

Practical Radiobiology for Proton Therapy Planning

Bleddyn Jones

Chapter 1

Particle physics for biological interactions

1.1 Physical beam parameters, essential dosimetry and reference (or control) radiation requirements for RBE studies

This chapter, intended more for the benefit of biologists rather than physicists, includes a short qualitative description of the physics base of photon and particle therapy, including linear energy transfer (LET) and its variants, and finally the choice of the control or reference radiation for relative biological effect (RBE) studies. It is assumed that the reader will be familiar with Bragg peaks and how these peaks are spread out to cover a defined clinical target volume. A comprehensive account of the physics of proton therapy by Newhauser and Zhang (2015) is appropriate only for physicists, but their figure 15 on page 179 is reproduced here as figure 1.1, and shows the dose (D) for multiple Bragg peaks obtained by using different proton energies, resulting in peaks at different depths (indicated by z on the abscissa) to form a plateau of relatively uniform dose when they are all summated. It should be noted that the flat section of the green line is composed of low LET radiation with the high LET being within the Bragg peak and the maximum LET at its end. The reader is encouraged to refer to this diagram while reading this chapter.

First, it is necessary to understand the basic concepts that underpin radiation dosimetry and the important differences between photon and positive charged particle therapies. For those less familiar with radiotherapy physics, or who wish to revise the key aspects, a brief summary is provided, concentrating on important definitions that lead up to the concept of LET, and its various forms. For more complete descriptions the reader should consult standard textbooks.

Radiation fluence refers to the number of radiation beamlets (or individual tracks) (N) within a beam which crosses the unit surface area, that is N/A, where A is the area covered by the whole beam, and so the units are cm^{-2}.

KERMA signifies the kinetic energy released per unit mass of a specified mass of medium, by release of secondary particles such as δ-rays and all ionisation products.

doi:10.1088/978-0-7503-1338-4ch1

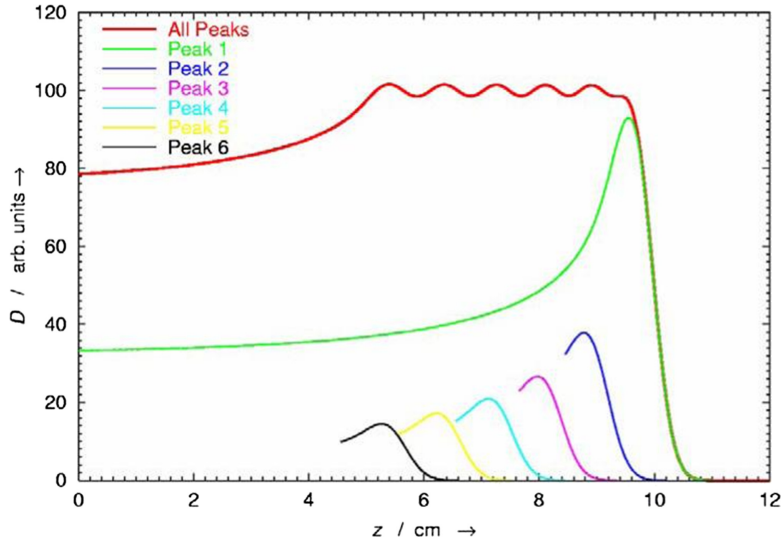

Figure 1.1. Absorbed dose D is shown as a function of depth z in water from a spread-out Bragg peak (SOBP) (uppermost curve) and its constituent pristine Bragg peaks (for the lower curves, for clarity; all but the deepest pristine Bragg peak are only partly drawn). In many cases, the clinical target volume is larger than the width of a pristine Bragg peak. By appropriately modulating the proton range by using different energies from the highest (peak 1), which provides dose to the greatest depth, and then with progressively reduced energies to provide peaks at each of the lower depths, the lowest energy providing peak 6. The fluence (here proportional to the height of each peak) is also varied in order to provide the intended uniform dose to the target, although in this example there is some undulation of the 'all peaks' summated dose from each separate energy contribution because of the low number of peaks used for illustrative purposes. Reproduced from Newhauser and Zhang (2015).

However, some of the energy released (in J Kg^{-1}) will be sufficient to pass beyond the volume of the mass of interest and be absorbed elsewhere. Consequently it was necessary for the physicist L H Gray to define the **absorbed dose** as the energy absorbed by a mass of interest, again as J Kg^{-1}, which should include not only the primary ionisation events, but also all secondary particles, such as δ-rays, neutrons, recoiled neutrons/protons and fragmented ions, that make a contribution.

Most dose calculations are performed for unit density water, so mass and volume have the same number. For denser structures, such as bone or lower density air cavities, the absorbed dose is larger and smaller, respectively, and is often assumed to be mainly dependent on electron density in the case of megavoltage x-rays (photons) in the most commonly used clinical range (4–8 MeV). Lower energy x-rays (especially below 100 keV, which may form part of the x-ray spectrum from x-ray generators that have higher peak energies such as 200–300 keV) cause ionisation by the photoelectric effect in proportion to the atomic charge cubed (i.e. Z^3). In contrast, uncharged fast neutrons preferentially interact with neutron deficient nuclei such as hydrogen, producing recoil protons, so that richly hydrogenated compounds, such as lipid rich tissues (such as myelin in brain white matter and fat) have a greater KERMA than water.

To arrive at the absorbed dose, use is made of energy transfer coefficients and radiation absorption parameters. It is important to note that the loss of dose with depth for divergent radiation, for example x-rays emanating from a high-Z metal target, are mostly due to inverse square law (ISL) effects as well as due to tissue absorption. For highly collimated beams, such as pencil beams, ISL effects are much reduced.

Particle beams may be delivered as pencil beams, but may also be passively scattered with resultant divergence and ISL effects. There is a further divergence effect in all cases, caused by coulombic force scattering of similarly positively charged particles (when stripped of their electrons), which also depends on their energy and mass (each of which reduces the scattering when large). The resultant diversion of the beam with tissue depth reduces the fluence.

In particle therapy the intended absorbed dose is normally prescribed as an equivalent dose. This can cause confusion to practitioners, since the equivalent dose has been expressed in different ways, for example the cobalt equivalent Gy, or Gy equivalent (or eq-Gy), or Gy-RBE or RBE-Gy, where the particle dose has been reduced by the working RBE value in order to achieve the same intended effect as from, say, megavoltage x-rays or photons. Further confusion is caused by the standard expression for equivalent Gy, for example, as

$$\text{Gy–RBE absorbed dose} = \text{particle absorbed dose} \times \text{RBE},$$

but it is important to realise and understand the re-arrangement, which is used in practice, as

$$\text{particle absorbed dose} = \text{Gy–RBE absorbed dose} \div \text{RBE}.$$

The physician chooses the most appropriate eq-Gy (or RBE Gy) dose of photons (or x-rays); this is then divided by the RBE to provide the physical absorbed dose of particles given to the patient.

Very recently, the ICRU has decided not to continue the use of the RBE-Gy, which was especially associated with the constant 1.1 RBE used for proton therapy. Doses should now be specified in Gy for each radiation modality, which will allow better identification of RBE values in the future.

In routine clinical megavoltage x-ray (photon) therapy, the ionisation is relatively uniform along the radiation track. The depth dose curve for a monoenergetic and non-divergent beam shows a fairly constant fractional loss of absorbed dose per unit distance traversed from its initial maximum ($d_{\max}$) dose so that at deeper distances (denoted by x) the dose d_x can be approximated as $d_x = d_{\max}\mathrm{e}^{-\mu x}$, where μ is the attenuation coefficient. The same is not true along a charged particle beam since slowing of the particle increases the energy loss (E) per unit distance (x), denoted by $\mathrm{d}E/\mathrm{d}x$. This is because of the increasing probability that opposite coulombic charges will interact, causing more ionisation and so increased KERMA and locally absorbed dose, the extreme case being at the distal part of the Bragg peak itself. Since the ionisation probability changes with depth it is useful to consider a further parameter, the LET, which reflects the closeness of local ionisations along a beam track. LET is not only relevant to charged particles but also to low energy

photons/x-rays since whenever photon energy falls to the keV range their secondary particles have lower energy and a higher LET.

LET is defined as the energy lost per unit length of medium by a charged particle (as, e.g., 1 keV μm^{-1}, or 1.602 J m^{-1}). There are several variants of LET such as the following.

1. L_Δ, where Δ refers to the maximum limit of energy (e.g. L_{100} would consider only energies below 100 keV μm^{-1}) and LET as total energy loss (L_∞). This latter parameter reflects 'stopping power' in the medium, and so includes its density, with units expressed as MeV cm^2 g^{-1}, or J m^2 kg^{-1}.
2. If there are different energies in a beam, as might be the case with fast neutrons or SOBP charged particles, a LET spectrum can be used, calculated as either 'track average' or as 'absorbed dose average' (or energy average) LET.
3. In microdosimetry, the unsatisfactory aspects of 'average LET' are often overcome by graphical presentations of LET plotted against the dose fraction per log LET interval.
4. The lineal energy (y), which takes account stochastic energy deposition (whereas LET does not). This is defined as $y = \varepsilon/d_{av}$, where ε is the energy imparted in a volume with d_{av} being the mean track chord length in the volume.
5. The final variant, with attractive properties for bio-molecular considerations, is to account for δ-rays ejected from tracks. These δ-rays are radially distributed and responsible for most bio-effects and ionisations collected by detectors. With considerable acumen, Katz *et al* (1971) proposed the use of $Z^{*2}\beta^{-2}$, where Z^* is the effective nuclear charge of the atomic nucleus of atomic charge Z and β is the relativistic velocity (v/c), in order to estimate the effective radius of ionisation, which should correlate with bio-effectiveness. It must be realised that, as fully stripped ions slow down, they pick up electrons while causing ionisation, so Z^* becomes less than Z, the parameter will change with depth. This is discussed further in chapter 8.

The loss of energy E with distance in a medium is well described by the Bethe Bloch equation:

$$-\frac{\mathrm{d}E}{\mathrm{d}x} = \frac{4\pi}{m_e c^2}\frac{nz^2}{\beta^2}\left(\frac{e^2}{4\pi\epsilon_0}\right)^2\left[\ln\left(\frac{2m_e c^2\beta^2}{I(1-\beta^2)}\right) - \beta^2\right].$$

For the purpose of understanding, this formidable formulation can be reduced to:

$$-\mathrm{d}E/\mathrm{d}x\ (\text{energy/cm}) = K\ (\text{charge}^2/\text{velocity}^2),$$

where K replaces the constant physical parameters. It can easily be seen that, for a proton (charge = 1), or carbon (charge = 6, if all electrons are stripped away), the energy loss will depend on the Z number but will increase sharply as velocity falls. This occurs as particles slow down through a medium. After such slowing they interact with orbital electrons in nearby molecules and cause ionisation. The Bragg peak represents a sharp rise in $\mathrm{d}E/\mathrm{d}x$ with loss of velocity or energy at increasing depth. The initial energy or velocity will govern the complete range (or depth) of

energy deposition, so beams with higher incident energies at the level of the skin will have Bragg peaks at greater depths.

1.1.1 Straggling and fragmentation

This term is used to describe the variation in path length caused by differences in energy and velocity reduction through a medium or tissue, due largely to differences in interactions along the beam path due to variations in electron density/tissue composition and other stochastic events. It normally denotes a blurring-like effect on the beam towards its distal edge, but there is also some degree of lateral straggling for particles that are more easily scattered. Thus, the beam edge is not so sharp with protons, which are lighter than helium or carbon ions. For even heavier ions, such as carbon, there is a distinct fragmentation tail caused by nuclear interactions and emitted γ-rays, which results in a tail of dose beyond the end of the Bragg peaks. For lighter particles, such as protons, fragmented ions do not occur but, as with heavier particles, the tissue interactions can cause emission of γ-rays and some neutrons.

1.1.2 Separation of charged particles with increasing tissue depth

The coulombic forces due to the nuclear charge will cause charged particles to separate from each other gradually in proportion to their tissue depth, and also in inverse proportion to their mass and velocity. This will occur in a beam traversing a vacuum. This is often referred to as 'coulombic scattering', but in matter will also include much wider angle scattering due to repulsive charge interactions with atomic nuclei (as in the classical example of Rutherford scattering). So, protons (charge = 1, mass unit = 1) will separate less than electrons (charge = 1, mass $\approx$ 1/2000 of mass unit), Compared to protons, heavier ions (also containing neutrons so they have mass greater than their Z number) show lesser deviation despite their increased charge, even if fully 'stripped' of electrons before their acceleration, although some particles will gain electrons during their transit through matter.

There appears to be no formal term that describes the average or median inter-track separation distances, which may contribute to biological effect changes over and above the LET, as discussed below. It is easy to crudely estimate the mean inter-track separation distance (s) by the following basic approach (see figure 1.2).

The overall area A is divided by the number of tracks to provide A/N, the average area surrounding each track; if this is assumed to be a small square area (represented by s^2), then $A/N = s^2$. If, on average, the track occupies the centre of each square, then the average track separation will be s, which is $\sqrt{(A/N)}$, and which can also be expressed as $\sqrt{\frac{1}{F}}$, where F is the fluence (defined above). This might be an important parameter to use in the analysis of cell-survival studies and treatment outcomes, as it could modify the effect of LET and dose. For example, even if the LET parameter is calculated to be the same at, say, the mid-Bragg peak for the same particle type but accelerated to two quite different energies resulting in Bragg peaks at two different depths (where the particle energies will then be the same), any reduction in bio-effectiveness could be due to greater separation of tracks in the case of the particles

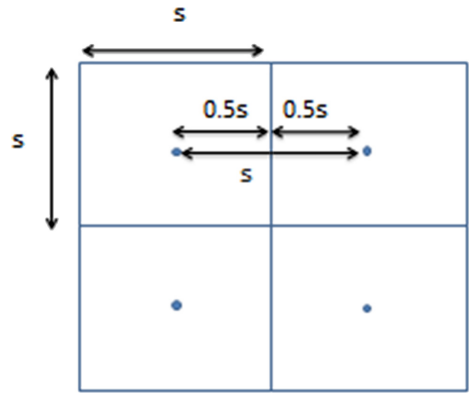

Figure 1.2. Four particle tracks are represented in cross section by central points within a square of side s; the inter-track distance is then s. For N tracks, the overall area (A) is Ns^2.

that were accelerated to the higher energy. Such a process would depend on increasing track separation due to coulombic scattering, and even more so on the deliberate use of scattering filters, causing ISL geometric dispersion of the beam at increasing depths.

This can be further expressed in a very simple way. Consider tracks of radius a, with volume $\pi a^2 x$ when considered as a cylinder extending to depth x. The inter-track distance is s, so that the fractional volume occupied by a single track compared with its surrounding volume of $s^2 x$ is

$$\frac{\pi a^2 x}{s^2 x} = \frac{\pi a^2 N}{A} = \pi a^2 F$$

(since $s^2 = 1/F = A/N$).

For the same fluence, as the overall area (A) of a beam reduces, the closeness of tracks per unit area (and volume) increases. But if A increases, the fluence falls and the closeness of tracks decreases. For different ions the specific Katz track radius may be used.

Such an effect can actually be visualised using GEANT4 and FLUKA in-silico simulations, shown to the author by Dr David Colling (Imperial College) and Dr Francesca Fiorini (Oxford), respectively. Although LET may be similar for each track at each depth, their increased separation may be sufficient to diminish the bio-effect since more cell nuclear material or even whole cells may be un-irradiated. Some evidence for reduced bio-effectiveness with depth in the case of passively scattered beams is given below.

1.1.3 Particle accelerators

Synchrotrons and cyclotrons are the commonest accelerators used for charged particle medical beams. These terms can confuse since modern cyclotrons are in fact synchro-cyclotrons, but the more basic nomenclature remains useful. Printing space does not permit a full description of these. For a summary of how these accelerators

operate the reader should refer to short accounts such as Peach *et al* (2011), designed for hospital readers, with more complete accounts by Wilson (2001) in his excellent textbook, which contains ample worked examples concerning beam control, etc. Suffice it to say here that cyclotrons operating from a circular cavity arrangement accelerate protons to their peak energy on extraction. To produce lower energies that result in Bragg peaks at depths less than the maximum range, the beam must be degraded within metal or plastic strips of differing thicknesses (which become highly radioactive and must be situated sufficiently remote from the patient because of induced radiation including neutrons). Cyclotrons deliver high dose rates (0.5–1 Gy s^{-1}). For example 12 Gy in 24 s is not unusual.

In contrast, synchrotrons, which are used to accelerate protons or particles heavier than helium, occupy a much larger floor space and operate by a single radiofrequency accelerator combined with magnetic focusing and defocusing bending the beam around a geometrical arrangement of magnets, which leads the beam back to the original point for further acceleration. The magnetic field strength must be carefully increased to match the particle energies at each 'cycle'. When the desired energy is obtained the 'particle bunch' is extracted and then delivered.

There are two options for controlling beam size: the pencil beams delivered from the accelerator can be passively scattered by a filter to a wider area, but with a small neutron contamination, depending on the efficiency and composition of the filter. The alternative is to use the pencil beam and magnetically deflect the beam to the positions required (active scanning), which avoids neutron production and provides better conformity of dose to the intended targets.

In each case the energies delivered from these accelerators have a spread in terms of energy and in spatial properties. There are some useful terms to denote these.

Luminosity refers to the total energy emitted, often expressed per unit time.

Emittance measures the average spread of particle coordinates with respect to their position in 3D space and their momentum, with dimensions of length (e.g. metres) or length times angle (metres times radians). In a low-emittance particle beam, the particles are confined to a small distance and have nearly the same momentum. The probability of particle interactions will be greater, resulting in higher luminosity.

Also, further beam parameters include energy spread (in standard deviations), pulse repetition rate (f), bunches per macropulse (Mb) and effective bunch rate (fMb).

Proton range uncertainties

The energy spread of protons, their interactions in non-homogenous tissue, as well as physiological movement of tissues, all contribute to range uncertainties caused by variations in Bragg peak positions. These uncertainties will vary, depending on anatomical site, from millimetres to several centimetres (in the case of physiological movements such as breathing). Patient positioning variations, gain or loss of weight during treatment, with resultant changes in subcutaneous fat depths and tumour shrinkage, can all critically affect particle range, dose and LET distribution, with implications for tumour control and toxicities. Imaging of the Bragg peak position is

improving; for example proton nuclear activation of positron emitting isotopes within the body results in PET scanning signal detection to an accuracy of around 2 mm.

A clinical example of some of these considerations, and RBE allocation uncertainties, are shown in figure 2 in Jones (2015) (available on open access). This example illustrates the interdependence of dose, LET and RBE on the potential clinical outcomes. The proton 'dose' shown was calculated using an RBE conversion factor of 1.1 (the equivalent x-ray dose is divided by 1.1). The required 76 Gy dose to the target volume is achieved in both cases, but the proton plan spares the heart, a considerable volume of lung, and breast tissue, so reducing the later risk of breathlessness on exertion, sudden cardiac death and of radiation-induced breast cancer. The small ringed area anterior to the high dose volume shows the position of the spinal cord and the dose received by this structure appears to be same for both treatment plans. Despite these attractive features, what if the RBE of 1.1 used in the dose prescription is higher than that of the tumour and lower than that of the spinal cord? Then, there would be enhanced risks of both tumour recurrence and spinal damage (resulting in paralysis of the lower limbs) when compared with the x-ray based treatment. Also, the effect of increasing particle range, as might happen in a patient with weight loss (so reducing the subcutaneous fat and allowing the beam to travel further), might lead to higher LET and dose in the spinal cord, increasing the risk of paralysis, while also lowering the LET and dose to the tumour, so reducing the probability of tumour control. Weight gain may cause the opposite effects. The simplest allowance for changes in tissue distances would be to allow millimetre exchanges, assuming uniform tissue density. In this way each millimetre lost or gained will shift the high dose boundary in either direction by the same amount. The ballistic advantages, changes in dose distribution and these more uncertain aspects of proton beam therapy (PBT) should be mentioned in informed consent procedures to patients, with explanation of how these risks can be minimised.

To reduce range instabilities, meticulous daily assessment of patient dimensions, accurate tumour localisation, patient immobilisation, etc, including confirmatory measurements made by non-ionising techniques such as ultrasonography, are necessary requirements. Improved dose computing techniques and 4D planning (the three dimensions of space and the fourth of time is included), including adaptive techniques to changes in normal tissues and tumour positions/dimensions with time are even more important in PBT than conventional radiotherapy. Further details of these techniques, including proton radiography, are available elsewhere.

There has always been concern that the highest LET and RBE will occur towards the end of the particle range, even if the Bragg peaks are 'spread out' by the use of range filters or by the spot scanning method. This is because of the greater proportion of high LET radiation in the distal part of the beam; more proximal sections have a lower average LET due to a greater proportion of low LET in the non-plateau section of the SOBPs. The distal end will have the highest LET, which might lead to unintended clinical effects. This concern has led to the intelligent use of 'patch field' techniques, which aligns lateral beam edges (rather than distal edges) against sensitive anatomical structures when using passive beam scattering. In

contrast, lateral beam edge beam uncertainties are not so well understood. Beams diverge with depth due to coulomb scattering, and there is geometric divergence with passively scattered beams. Lateral scatter must carry implications for higher LET values, since deviated particles will form Bragg peaks in a more lateral direction. Also, the tracks become more separated and less linear, so a more microvolumetric assessment of energy transfer (MVET) is indicated, as well as the number of particles per unit volume, related to the inter-track distances explained above. There is already evidence that with spot-scanned intensity modulated proton therapy high LET values can be found outside the tumour-bearing target volumes. This is perhaps explained by a greater proportion of partially overlapping beam edges, along with the additional weighting applied to some beamlets, and the smaller inter-track distances.

In the case of carbon ions, the dose profile of each single field (composed of multiple Bragg peaks, as in figure 1.1) was designed to compensate for the inevitable increase in LET along its path (Kanai *et al* 1997): deeper regions, where LET is highest, receive a lower dose; shallower regions are allowed a higher dose because of the lower prevalent LET. Such an elegant arrangement has not been used for proton beams, but should be an urgent consideration, especially when single- or few-field directions are used and if important functional normal tissue is exposed at these distal beam regions. Confirmation of a marked increase in the RBE for lung fibrosis in patients treated by single SOBP proton fields has increased this concern (Underwood 2017). The weighting of proton dose towards the distal end of the beam should be reduced to compensate for such an effect, although the extent will need to be determined by the dose per fraction used, using LET-RBE models, as described in chapters 8 and 9.

1.2 Physics interacting with biology

1.2.1 RBE

The study of the RBE of different radiation qualities is important, since the RBE concept is used in the dose prescription process of hadrontherapy. RBE is defined as:

$$\text{RBE} = \frac{\text{dose of control (low LET) radiation}}{\text{dose of test (higher LET) hadron radiation}}$$

for the same bio-effect, using each class of radiation.

The numerator dose becomes the number by which RBE is scaled from values of one upwards, the denominator being less than the numerator.

The RBE is dependent on the LET of the radiation, with an initial increase in RBE being followed by a reduction at higher LET values due to overkill/or cell killing inefficiency, the turnover point being dependent on the nuclear charge (z) of the ion, but not, apparently, the cell type. The RBE is also inversely related to dose for reasons related to differences in cellular radiosensitivities and the slope of the effectiveness curves between the reference (or control) low LET radiation and the higher LET state. This is illustrated in figure 1.3, based on the linear quadratic model of radiation effect (E) where $E = \alpha d + \beta d^2$, d being the dose, α and β are

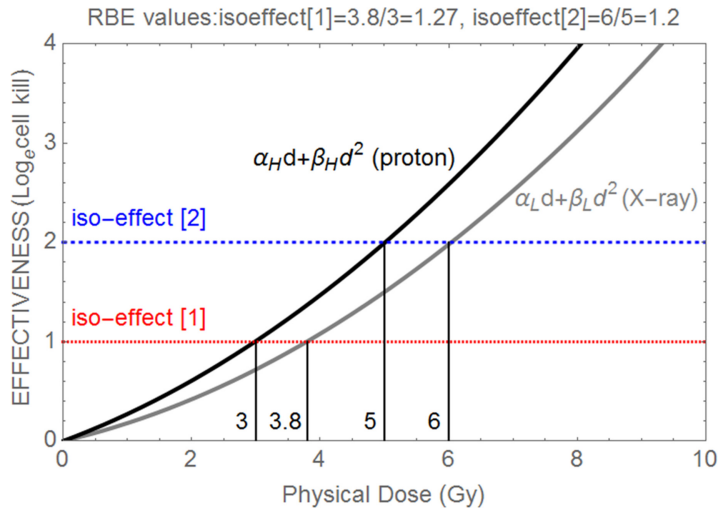

Figure 1.3. Demonstration of the RBE principle for two dose effectiveness curves produced by x-rays (photons) and protons (assuming $\alpha_L = 0.15$ Gy^{-1}, $\alpha_H = 0.24$ Gy^{-1}, $\beta_L = 0.03$ Gy^{-2}, $\beta_H = 0.032$ Gy^{-2}) and where two different iso-effect levels (1 and 2) are considered; their corresponding RBEs are also shown. The numbers 3, 3.8, 5 and 6 refer to the physical doses at which each iso-effect line meets each curve, respectively; d_H followed by d_L for iso-effect 1, d_H and d_L for iso-effect 2. The RBE is given by d_L/d_H in each case, as shown above the figure frame. Reproduced from Jones (2017).

biological coefficients, with subscripts L and H for the low and high LET states; further details regarding the radiobiology are given in following chapters. The RBE falls from 1.27 to 1.2 due to the geometry of the curves and such a change is an inherent feature of the linear-quadratic model providing that the LET-induced increment in α exceeds that in β (further discussed in chapters 8 and 9).

The RBE concept was included in the dose prescription system for fast neutron therapy and continues to be important in proton and ion beam therapy; it is also potentially relevant in nuclear medicine and some forms of brachytherapy, but has not yet been used in their clinical application.

In experiments to determine the RBE, the choice of the control (or reference) radiation has varied considerably; examples include low-voltage x-rays (100–200 keV peak) and orthovoltage (200–350 keV peak), along with variable degrees of filtration to remove the lowermost keV x-rays within the x-ray spectrum. Other examples include 137-caesium or 60-Co gamma rays, megavoltage electrons and, more rarely, megavoltage x-rays in the clinical range 4–10 MeV. The lower the energy of any beam, the greater the LET; this applies to x- and γ-rays, protons, and all ions and electrons, because lower energies result in more localised energy release and absorption, and a higher LET, and also results in more clustered DNA damage. This will increase the RBE up to a saturation level beyond which the RBE falls at even higher LET values. Conversely, at higher energies of a particle or photon beam, then local LET and RBE are reduced, because the ionisations are not so spatially clustered.

Since the reference radiation (sometimes called the control radiation) supplies the numerator dose for the RBE estimation, this must exceed the hadron radiation dose for the same bio-effect in order for the RBE to be greater than one. Should the control RBE irradiator have an LET that is greater than the test hadron LET then the RBE will be less than one. Choosing a control irradiator that has a higher LET than that of the photons/x-rays used in hospital clinics, will give a lower estimate of RBE than would be the case in the hospital setting for the same cellular system.

1.2.2 Choice of the control (or reference) radiation source

It follows that the choice of the reference radiation will have an important effect on the RBE ratio found. For example Hall and Gaccia (2011) quote typical LET values (keV μm^{-1}) of 2 for 250 keV (but the filtration is unspecified), 0.2 for 60-Co, 4.7 for 10 MeV protons and 0.5 for 150 MeV protons, while megavoltage photons are not mentioned. More comprehensive, but still incomplete, data can be found in ICRU report 16 (1970). These suggest, by extrapolation, that megavoltage photons in the clinical range of 4–8 MeV would have a LET value of around 0.2 keV μm^{-1}. A useful collation of data in Andrews (1978) shows a mean LET of 0.5 keV μm^{-1} for 3 MeV photons and 60-cobalt irradiation, but stopping powers (or LET_{∞}) of 0.18 for 2 MeV electrons as well as being the theoretical minimum for any charged particle, and hence an important limit or baseline for relative biological effect studies. The average Compton electrons produced from 60-cobalt γ-rays have an LET_{∞} of 0.26 keV μm^{-1}, so a slightly lower value around 0.2 keV μm^{-1} would be expected from clinical range megavoltage photons.

Further information is contained in some publications, such as Spadinger and Palcic (1992), where an LET range of 5.5–6 keV μm^{-1} is quoted for 25 keV x-rays and 1.7 keV μm^{-1} for 122 KeV x-rays (the average value obtained with 250 KeV x-rays with 0.35 mm Cu and 0.4 mm Sn filtration), with a value of 0.2 keV μm^{-1} for 11 MeV electrons, which are likely to closely resemble megavoltage photons in the clinical range.

From the above data, it seems reasonable to use a control radiation of either electrons of photons, according to the experiment being done, with an LET value of around 0.2 keV μm^{-1}, as would be achieved with a clinical photon or electron beam. The added value of having a megavoltage photon beam would be for comparative combined ballistic and radiobiological studies in humanoid phantoms between charged particles and clinically relevant photon energies.

Some important examples of the unsuitability of orthovoltage and lower voltage x-rays beams as the control/reference radiation are as follows.

1. For the collated proton RBE data of Paganetti *et al* (2002), orthovoltage radiations, 14 low voltage or orthovoltage x-ray irradiations had an RBE of less than one and only one such experiment showed an RBE of just over one. The probability of this being due to chance or experimental error is low; use of the sign test provides the probability of there being no difference as $p = 0.00061$, a highly significant result.

2. The literature contains a report by Amols *et al* (1986) who measured cell survival data in DLD-1 human tumour cells. Their results clearly demonstrate a statistically significant RBE difference between orthovoltage and megavoltage radiation ($p = 0.001$). A small difference was also measured in the RBE between megavoltage photons and megavoltage electrons, but the difference was not statistically significant ($p = 0.25$). All biological, dosimetric, and microdosimetric data were obtained under nearly identical geometric conditions, but using only one cell line.

The past literature contains many contributions that concentrate on the influence of lower photon energies in the low kilovoltage range on the RBE, but these are mainly in the context of radiation protection, because this class of x-rays are used so much in routine diagnostic medicine. Such work has confirmed that the RBE varies inversely with photon and particle energy (see, for example, the review by Hill 2004).

The RBE should be taken into account in clinical radiotherapy using positively charged particle beams, where RBEs can be significant even in the case of protons. Papers by Belli *et al* (2000), Britten *et al* (2013) and Marshall *et al* (2016), are examples of such work, containing well-documented experimental detail. There is presently a potential shift of opinion to include more flexible (or variable) RBE values than the constant values previously assumed in proton therapy, in order not to: (a) under-dose certain radiosensitive tumour classes and (b) over-dose late-reacting normal tissues of clinical importance. This is discussed in later chapters.

The urgent need to clarify RBEs in critical experimental normal tissues exposed to proton and other ionic beams will require careful choice of control radiation if the purpose of such studies is to provide information that will ultimately be useful for clinical purposes. Some potential forms of control radiations can easily be eliminated, as is the case for orthovoltage x-rays, despite their low expense and convenience, should be avoided, since they will lead to lower estimates of the RBE. 60-cobalt units also have some significant disadvantages. These include lower dose rates with time, since it is advisable to use the same exposure times (within differences of only 1–2 min at the most) for the control and test irradiations, due to ongoing repair of sub-lethal radiation damage. Longer treatments will have slightly lower bio-effectiveness and this will influence the estimated RBE ratio. Also, the need to compensate for radioactive decay on a weekly or monthly basis may sometimes be forgotten or wrongly applied; the LET can be lower than for megavoltage photons and there is drift of dose rate with time, and modification of source treatment distances to compensate for radiation decay, with accompanying changes in depth dose distributions. There are also problems associated with radiation protection of staff, shielding requirements, and source replacements required with time, are expensive, and have their own difficulties.

Some laboratories do have a 137-caesium irradiator, which is more compact, and delivers monoenergetic photons close to 0.5 MeV, which should have an LET close to that of cobalt beams. Again radioactive decay has to be compensated for and dose rate effects may accrue with time, although this can be overcome by using shorter

source to target distances. Such a unit can be fitted into the size occupied by a large double refrigerator without additional shielding.

Megavoltage electrons are a reasonable choice for the control radiation in RBE studies. However, electron dosimetry, although much improved in recent years, has limitations due to its high scatter, especially for small field sizes, as well as an energy-dependent relationship of electron build-up with depth, which must be taken into account in any laboratory experiment. Electron fields are essentially SOBPs, often with lower RBEs than fields in megavoltage electron plateau regions, but there remains uncertainty as to their higher RBE values with fall off of dose and energy towards their end of range. It must not be forgotten that Auger electrons (from low energy radioactive emissions) can have very high RBEs. However a broad electron beam operating at, say, 8–10 MeV would give a satisfactory uniform dose for radiobiological experiments, but could not be used for beam ballistics combined with radiobiology comparisons.

There is interest in some particle therapy centres across Europe, including international laboratories like CERN, in addressing the clinically important RBE issue. For comparable results it is very important that the control radiation be standardised. The best standard to choose, despite the additional expense, would undoubtedly be megavoltage x-rays from a linear accelerator operating at typical energies used in the clinic. It is already the case that national radiation standards laboratories such NPL (Teddington, UK) contain a standard hospital linear accelerator for dosimetry comparisons and maintenance of standards. Likewise, laboratories that aim to contribute useful RBE data should use a control megavoltage linear accelerator with optional use of 4–10 MeV photons or electrons for their studies. A single 137-caesium source could also be useful.

Interestingly, since hospital linear accelerators are normally replaced every 10 years, it is relatively easy to obtain one that can be refurbished for experimental use. These would have a gantry for variable beam angles and collimation down to small field sizes.

1.2.3 Does the RBE reduce with depth in scattered beams?

In general, the RBE increases with depth due to the progressive increase in LET, especially within the Bragg peaks. However, there is evidence that if the same LET and dose is given at the same SOBP positions situated at markedly different depths, achieved by using a different incident energy, then the RBE is reduced in the deepest position. These intriguing experiments, led by V Megnin-Chanet (Institute Curie), were designed to study proton RBEs at various depths using the Orsay proton beams (Calugaru *et al* 2011), with two different incident energies of 76 and 201 MeV, with mid SOBPs at 20.5 and 160 mm, respectively, and also near the distal end of SOBPs at 26.9 and 185 mm, respectively, with identical LET characteristics towards their distal ends. The main physical differences appeared to be the beam widths: 3 and 12 cm diameters, respectively, indicating greater lateral dispersion at the increased depth after passive beam scattering. They observed a reduction in the RBE in two human cell lines from around the highest RBEs of 1.3–1.33 (at 3 cm depth) down to

1.0 (at 12 cm depth). Although the dose rates did differ with increasing depth, when DNA repair kinetics are considered the changes in minutes required to deliver the dose ranges used cannot account for the change in the RBE (the dose rate effect is discussed further in chapter 2).

In contrast, Britten *et al* (2013) found no such effect in two cell lines with incident energies of 87 and 200 MeV at Bloomington, where scanned beams were used. Scanned beams, without metallic filter-related scatter, essentially consist of parallel tracks and so deliver the shorter inter-track separation distance (s) over most of their range. They exhibit little geometric dispersion, so s is relatively well preserved with depth, only being affected by mild coulombic scattering, which manifests itself mostly near to the extreme range when energy and velocity are reduced. Alternative explanations for the findings of the Paris and Bloomington experiments might include chance, or a cellular batch effect, or the cell types used. These latter hypotheses are unlikely, as each Institute had used two different cell lines with different radiobiological properties.

The most obvious physical explanation of this phenomenon, although speculative, is the increasing track separation caused by divergence in passively scattered beams. There can also be an associated loss of RBE with depth owing to increasing γ-ray contributions, but these are small and would be at least partly offset by neutron production in matter, and this should be much the same in both centres. The geometric scattering from a metallic scattering foil will result in ISL effects, emerging from an apparent point source, so that radiation fluence will fall sharply with increasing distance or depth.

If it is assumed that the RBE is proportional to inter-track distance, which decreases with depth (x) in passively scattered beams, all other factors being equal (dose, energy, LET), and if the rate of change of this effect depends on the operative RBE, then

$$\mathrm{d}(\Delta\mathrm{RBE})/\mathrm{d}x = -K\Delta\mathrm{RBE},$$

where ΔRBE represents the RBE value in excess of 1.

Integration then provides, for RBE values >1, $1 + \mathrm{RBE}_x = 1 + \mathrm{RBE}_0\, \mathrm{e}^{-cx}$ where RBE_x is the RBE value in excess of 1 at a specified depth of x cm, RBE_0 is the RBE value in excess of 1 at the smallest depth, and c is a constant assumed to be controlled by track separation.

For the Megnin-Chanet experiments, and using their pooled data for two different human cell lines, the above function provides a value of $c = 0.009$ and 0.013, respectively, for the mid SOBP and distal SOBP positions used for the comparisons, and so it is possible to plot the reduction in the RBE with increasing depth, as shown in figure 1.4. Further experiments are required at multiple depths to confirm this hypothesis and achieve a more robust value for parameter c.

The other approach might be to use the inter-track distance (s). Using similar triangles, the radius of a divergent overall beam-field is proportional to the distance (x) that it traverses. For two different depth positions 1 and 2, indicated by the respective subscripts, the overall beam radii r_1 and r_2 are proportional to their respective depths (x_1 and x_2) due to the similar triangle rule; the areas A_1 and A_2 are

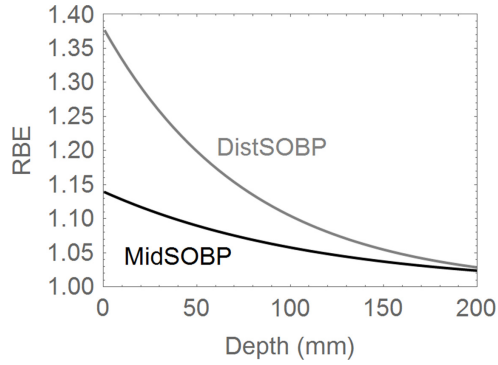

Figure 1.4. Putative relationship between the RBE and depth at the mid SOBP and distal SOBP obtained from data averaged for two human cell lines (HeLa and a head and neck squamous cell cancer line) for caesium and cobalt referenced RBE values obtained using the above equations.

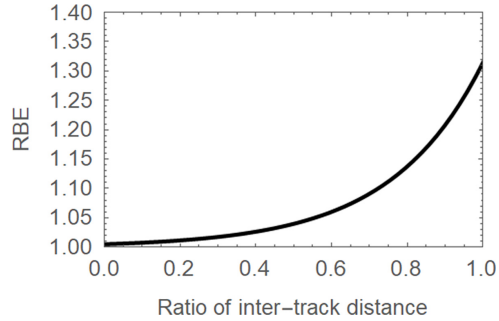

Figure 1.5. Plot of the RBE against the inter-track distance ratio (SR), normalised to $s = 1$ where the RBE is 1.33, but with an RBE close to 1 when the SR is around 0.1 for scattered proton beams, as in Calugaru *et al* (2011).

given by πr_1^2 and πr_2^2. The inter-track distance, when squared, is $s^2 = A/N$, and since N remains constant, then the ratio of inter-track distances (s_1/s_2) at two different depths will be the same as x_1/x_2. Using one of the data examples in Calugaru *et al* 2011, from $x = 2.69$ to 18.5 cm, the inter-track separation ratio (SR) will change from the shallowest depth, where s_1 is normalised to 1, down to $2.69/18.5 = 0.145$ (in the absence of precise knowledge of N or F). When this process is applied to the data, and by using a similar exponential function as in the above example, then the relationship between the RBE and the inter-track separation ratio (SR) can be expressed as $1 + 0.0055\ e^{(4.14SR)}$, and this function is plotted in figure 1.5.

Such exploratory data needs to be extended, with RBE estimations at many depths in a panel of cell lines in order to fully verify and extend this hypothesis, using further microdosimetry considerations.

Although speculative, if such a reduction in RBE with depth can occur in some cell lines with divergent beams, it may be possible to investigate reducing potential RBE problems in normal tissue adjacent to a tumour by electively increasing the path length (and energy) of the radiation and adding tissue equivalent material

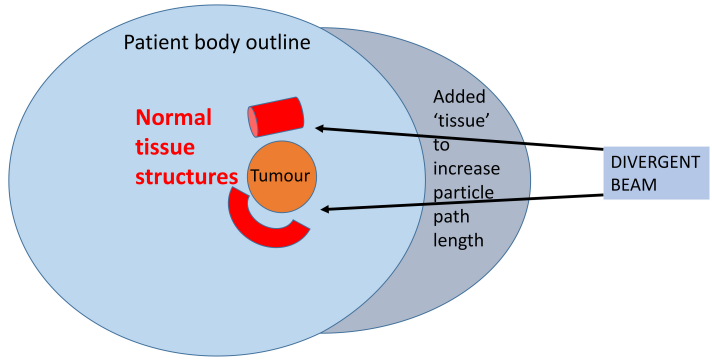

Figure 1.6. Potential treatment set up for deliberate reduction of RBE with depth using a longer treatment track distance by adding artificial 'tissue'.

outside the skin (as shown in figure 1.6), aiming for the RBE to be close to one at the critical distance. The length of additional material would require careful calculation to produce the SOBP at the required tissue depth, but with loss of the RBE this could be advantageous where the local biological characteristics confer a high normal tissue RBE in a critical structure and which exceeds any critical normal tissue dose sparing advantage. The alternative way of reducing the normal tissue RBE is to increase the dose per fraction of the particle therapy (these aspects are discussed in later chapters).

The possible detriment would be loss of electronic equilibrium build-up in skin and subcutaneous tissue due to the introduction of the artificial tissue, which allows the beam to diverge to the required extent to reduce the RBE.

References

Andrews J R 1978 *The Radiobiology of Human Cancer Radiotherapy* (Baltimore, MA: University Park) pp 241–4

Amols H I, Lagueux B and Cagna D 1986 Radiobiological effectiveness (RBE) of megavoltage x-ray and electron beams in radiotherapy *Radiat. Res.* **105** 58–67

Belli M *et al* 2000 Inactivation of human normal and tumour cells irradiated with low energy protons *Int. J. Radiat. Biol.* **76** 831–9

Britten R A *et al* 2013 Variations in the RBE for cell killing along the depth-dose profile of a modulated proton therapy beam *Radiat. Res.* **179** 21–8

Calugaru V, Nauraye C, Noël G, Giocanti N, Favaudon V and Mégnin-Chanet F 2011 Radiobiological characterization of two therapeutic proton beams with different initial energy spectra used at the Institut Curie Proton Therapy Center in Orsay. *Int. J. Radiat. Oncol. Biol. Phys.* **81** 1136–43

Hall E J and Giaccia A J 2012 *Radiobiology for the Radiologist* 7th edn (Philadelphia, PA: Kluwer/Lippincott Williams) p 106

Hill M A 2004 The variation in biological effectiveness of x-rays and gamma rays with energy *Radiat. Prot. Dosimetry.* **112** 471–81

ICRU Report 16 1970 *Linear Energy Transfer* (Bethesda, MD: ICRU)

Jones B 2015 Towards achieving the full clinical potential of proton therapy by inclusion of LET and RBE models *Cancers* **7** 460–80

Jones B 2017 Proton radiobiology and its clinical implications *ecancer* **11** 777

Kanai T, Furusawa Y, Fukutsu K, Itsukaichi H, Eguchi-Kasai K and Ohara H 1997 Irradiation of mixed beam and design of spread-out Bragg peak for heavy-ion radiotherapy *Radiat. Res.* **147** 78–85

Katz R, Ackerson B, Homoyooufar M and Sharma S C 1971 Inactivation of cells by heavy ion bombardment *Radiat. Res.* **47** 402–25

Marshall T I, Chaudhary P, Michaelidesová A, Vachelová J, Davídková M, Vondráček V, Schettino G and Prise K M 2016 Investigating the implications of a variable RBE on proton dose fractionation across a clinical pencil beam scanned spread-out Bragg peak *Int. J. Radiat. Oncol. Biol. Phys.* **95** 70–7

Newhauser W D and Zhang R 2015 The physics of proton therapy *Phys. Med. Biol.* **21** 155–209

Paganetti H, Niemierko A, Ancukiewicz M, Gerweck Le, Goitein M, Loeffler J S and Suit H D 2002 Relative biological effectiveness (RBE) values for proton beam therapy *Int. J. Radiat. Oncol. Biol. Phys.* **53** 407–21

Peach K, Wilson P and Jones B 2011 Accelerator science in medical physics *Brit. J. Radiol.* **84** S1–S10

Spadinger I and Palcic B 1992 The relative biological effectiveness of 60Co gamma-rays, 55 kVp x-rays, 250 kVp x-rays, and 11 MeV electrons at low doses *Int. J. Radiat. Biol.* **61** 345–53

Underwood T 2017 Oral presentation *Scott-Fowler Symposium, Oxford*, September 2017

Wilson E J N 2001 *An Introduction to Particle Accelerators* (Oxford: Clarendon)